ORIGINAL ARTICLE

WILEY

On stress/strain shielding and the material stiffness paradigm for dental implants

Raoof Korabi, MSc | Keren Shemtov-Yona, DDS, MSc | Daniel Rittel, PhD

Faculty of Mechanical Engineering, Technion, Haifa, 32000, Israel

Correspondence
Daniel Rittel, Faculty of Mechanical Engineering, Technion, Haifa, 32000, Israel.
Email: merittel@technion.ac.il

Abstract

Background: Stress shielding considerations suggest that the dental implant material's compliance should be matched to that of the host bone. However, this belief has not been confirmed from a general perspective, either clinically or numerically.

Purpose: To characterize the influence of the implant stiffness on its functionality using the failure envelope concept that examines all possible combinations of mechanical load and application angle for selected stress, strain and displacement-based bone failure criteria. Those criteria represent bone yielding, remodeling, and implant primary stability, respectively

Materials and methods: We performed numerical simulations to generate failure envelopes for all possible loading configurations of dental implants, with stiffness ranging from very low (polymer) to extremely high, through that of bone, titanium, and ceramics.

Results: Irrespective of the failure criterion, stiffer implants allow for improved implant functionality. The latter reduces with increasing compliance, while the trabecular bone experiences higher strains, albeit of an overall small level. Micromotions remain quite small irrespective of the implant's stiffness.

Conclusion: The current paradigm favoring reduced implant material's stiffness out of concern for stress or strain shielding, or even excessive micromotions, is not supported by the present calculations, that point exactly to the opposite.

KEYWORDS
failure envelope, finite element, implant material, micromotions, stress/strain shielding, Young's modulus

1 | INTRODUCTION

In the field of biomechanics, the concept of stress (or strain) shielding is a general term that describes the influence of an orthopedic implant on its surrounding bony tissue.[1,2] Bone cells are effective biosensors as they sense strain, whether due to tissue deformation, fluid flow in the cell matrix, or other processes by which the cells are deformed.

The level of a bone strain relates to the stimulus which leads to bone remodeling. High strain stimuli cause bone mass increases or changes in architecture, such as to increase the bone strength. By contrast, low strain stimuli (due to reduced activity) or disuse can cause bone loss or alterations in architecture that reduce bone strength.[3–5]

Stress or strain shielding in orthopedics stems from the concern that the extraneous implant may "shield" the bone from experiencing a desirable stress or strain level that is necessary for its remodeling. As an example, one can consider a long bone with a prosthetic plate. When the assembly experiences bending loads, the reinforcement plate stiffens the assembly so that the bone is not strained as it would without the plate. In such a situation, the bone is "shielded by the plate" in terms of the strains it experiences, and when the strain level becomes too low, the bone may resorb and this is undesirable.

While a relatively large body of research can be found in the field of long bone studies (eg, femur), as in Refs. 6–9, less is known in the field of implant dentistry where the emphasis has been put so far on implant design considerations or material selection issues,[10–13] noting

that Cilla and colleagues[6] recently expressed doubts on the influence of those 2 factors for hip prostheses.

Here, one should note the early study of Wiskott and Belser[14] who discussed the concept of stress shielding, and suggested that the straightforward extrapolation of this concept for long bones to the realm of dental implantology makes little sense. Their claim relies on the nature of the stresses and loading configuration experienced by a long reinforced bone, as opposed to an implant bearing jawbone, since the 2 cases are quite different in terms of loading.

As of today, most of the studies found in the literature, including the ones cited herein, consist of numerical simulations in which 2 stress or strain distributions are compared, namely before and after implantation, or simply corresponding to 2 or more designs and/or materials. One can indeed expect that the analysis of 2 totally different conditions, for example, with and without implant, will result is very different stress and strain distributions in the host bone. This is the general context in which the concept of shielding is currently understood and evoked.

It is also important to note that this concept becomes relevant *only once a criterion has been formulated* or adopted, that describes the response of the bone to the mechanical stimulus. In that respect, the widely accepted Wolff's law and mechanostat model[15–17] consider the bone strain as the relevant mechanical factor that dictates bone remodeling. More recently, Piccinini and colleagues[18] performed a joint clinical-numerical study and refined the concept to the identification of the equivalent (octahedral) shear strain as the specific factor in question.

If one sets aside the issue of implant geometrical design, a very actual question regarding shielding relates to the selection of *implant materials* such as ceramic[19] or polymers,[20] that differ significantly in their mechanical properties from those of the more conventional CP-titanium or alloys used in implant dentistry. One might even think of severely deformed commercially pure titanium severe plastic deformation (SPD),[21] whose tensile strength exceeds significantly that of the Ti6Al4V alloy.

Here, one can also set aside implant strength considerations, since whatever material is selected, it is not expected to fail as a result of monotonic overloading, while the bone is the component of the bone-implant system that should be scrutinized. In other words, the implant is not expected to reach its monotonic mechanical failure load, whereas the weak link in the implant-bone system is obviously the bone. Consequently, the relevant property for bone shielding considerations is the *elasticity of the implant material* as the factor that determines load transfer to the bone.

In the quest for materials whose modulus of elasticity comes closer to that of the bone, Stoppie and colleagues[20] performed a clinical and modeling study of 2 implant materials with radically different elasticity moduli, namely PEEK (polymer) and Titanium, for which the ratio of the Young's moduli is about 3%. While underlining the importance of the bone-implant interfacial parameters (also noted by Vaillancourt and colleagues[22]), the authors observed an improved osseointegration with the PEEK implants, which they attributed to its low modulus of elasticity and its influence on the peri-implant strains. In a recent study,

Piotrowski and colleagues[23] presented a thorough numerical study of the influence of Young's modulus on the bone field parameters. The reported results concern the cortical bone only, and among the study cases, one can find the Young's modulus of dentine which is treated as the reference material. The selected loading case is vertical only, with a fixed load (pressure) value applied on the implant. The authors conclude, like many previous studies, that in order to get as close as possible to the reference case, the Young's modulus of the implant has to be as close as possible to that of the reference bone/material, which is perfectly logical and in fact the current paradigm in the field. Let us note here that this conclusion stands somewhat at odds with the previous study of Vaillancourt and colleagues[22] who resorted to extremely low modulus materials as their best choice.

From the above-mentioned studies, it appears that the current paradigm is that lower Young's modulus materials are preferable for implant manufacturing. However, those conclusions lack generality for the reason that they only consider one, or at most 2 loading, particular configurations (angle and magnitude of the applied load). Moreover, while the concept of shielding is alluded to, it is not always clear what is the reference case with respect to which shielding is observed, and whether shielding applies to stresses, strains or even displacements in the host bone and at the bone-implant interface. Finally, while the cortical bone is obviously the main component to "suffer" from the loading (see eg, Ref. 24), one should also verify the fate of the trabecular bone.

Therefore, the main issue to be addressed in this work is that of the influence of the modulus of elasticity of a dental implant on the stress, strain and micromotions in the host bone, with emphasis on generality of the loading configuration (values and angles).

For this goal, we use the concept of failure envelope, recently proposed by Korabi and colleagues.[24] The failure envelope is defined as the locus of all admissible vertical and lateral loads that can be safely applied to the dental implant without exceeding the selected criterion for bone failure, be it stress, strain or strain energy density-based.

In other words, one does not perform a calculation to determine stresses, strains, and displacements in the host bone *for a specific load case*, but rather, one selects the bone failure criterion and calculates *all possible admissible load configurations* (value and angle) for the bone-implant assembly, namely the failure envelope. Within this concept, shielding is to be understood as the reduction (negative) or even increase (positive) of admissible loads in a comparative way.

For a fixed bone-dental implant geometry, this article presents a systematic numerical study of the influence of the modulus of elasticity of a dental implant on the jawbone, with reference to potential shielding effects. The investigated implant is (arbitrarily) assigned a modulus of elasticity of E/100, ~E/5, E/2, E, 2E, and 100E, respectively, with E being the Young's modulus of Titanium while all other parameters of the problem are fixed. Note that E/2, E, and 2E cover the broad range of engineering materials from polymers through metals and ceramics. The last case of the 100E material describes an extremely stiff imaginary material, while the E/100 case is an extremely soft polymer. The ~E/5 modulus has a special meaning as it represents the modulus of the cortical bone. We limit ourselves to 2 bone failure criteria: Strain
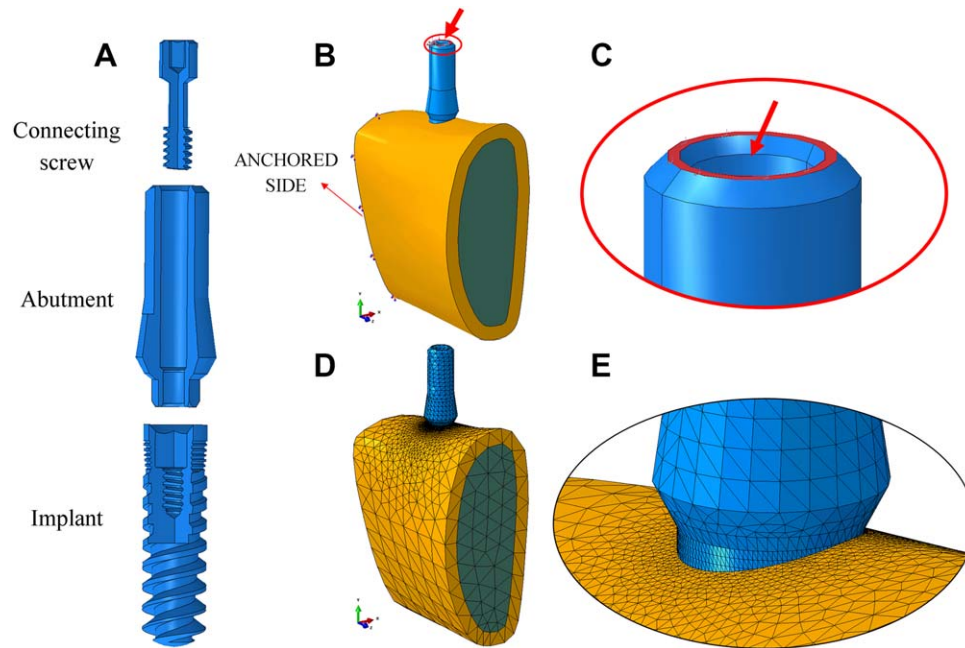
FIGURE 1 A, Implant system exploded view. B, Model assembly, including the bone cut section and implant system, with the boundary condition on each side of the bone. The area circled in red is the region where the loads were applied. C, Zoom in on the region where the loads where applied. D, Meshed model of the bone-implant model. E, Zoom in on the refined mesh near the implant-bone contact region

(mechanostat-based), and stress (bone yielding) considerations, and compare them in terms of failure envelopes.

In addition, we examine one specific loading case to assess the influence of the implant's stiffness on the bone-implant relative micro-motions.[5,14] Likewise, we examine the apical strains in the trabecular bone to assess any possible extensive damage in that region that might result from implant stiffness variations.

The first part of the article introduces the numerical model. The second part shows and compares the calculated failure envelopes based on octahedral shear strain,[18] and Tresca (shear) stress. Next, we present results about bone-implant micromotions and strains in the trabecular bone. The results are discussed, and the article ends with concluding remarks.

2 | MATERIALS AND METHODS

A bone section extracted from the mandible and implant system were modeled using finite element (FE) method under the assumption of small strain linear elasticity. The 3D nonlinear static analyses were carried out using the commercial code Abaqus.[25]

2.1 | Parts and material properties

The bone section geometry was acquired from the literature.[26] A section from the molar region between the first and third molars of the left side (shown in Figure 1B) was obtained. To account for the 2 bone macro-structures, a 2 mm thick cortical bone shell[27] was created, surrounding an internal trabecular bone. The last step was the insertion of the implant into the second molar location in the bone, and creating a

cut of its shape, resulting in a perfect geometrical fit between the implant's geometry and bone section used.

The selected implant system is very similar to a commercial implant (MIS Seven, http://www.misimplants.com/implants/brands/seven/seven-mf7-13375.html, Figure 1A). The implant has a 3.75 mm diameter near the neck and is 13 mm long, with 5 micro-rings near the top, where it is supposed to be in contact with the cortical bone. The implant features a conical shape with threads that reduce in thickness near the apical bottom.

The abutment Figure 1A, is 13 mm long, with a hexagonal connection at the bottom, that is designed to be inserted into a matching implant. Usually the crown is fitted on top of it, however to decrease the number of parts and save on computing time, the loads where applied directly on top of the abutment.

The connecting screw Figure 1A, is designed to hold the abutment and implant together, restricting any relative movement between them. The screw is 7.5 mm long.

All the parts used in this work were assigned a linear elastic, homogenous material model.

The *cortical* bone was assumed to be isotropic with its mechanical properties according to Ref. 28, listed in Table 1.

TABLE 1 Elastic mechanical properties of materials used in the FE model

Material	Young's modulus E (GPa)	Poisson's ratio υ
Ti-6Al-4V ELI	113.8	0.33
Isotropic cortical bone	19.7	0.30
Cancellous bone	0.056	0.34

The *trabecular* bone was also assumed to be isotropic, with mechanical properties according to Refs. 29 and [30], Table 1. The material model was simplified without impairing the accuracy of the results.[24]

Since the main purpose of this work was the effect of Young's modulus of the implant system on the bone stresses and strains, different isotropic mechanical properties where assigned to the implant system (implant, abutment, and connecting screw). Those properties could represent different engineering materials, ranging from soft polymers all the way to the toughest ceramics, and an extreme (imaginary) stiffness case. The selected moduli values were referred to that of Ti-6Al-4V ELI[31] (Table 1). The cases chosen in this work are: E (Ti-6Al-4V), E/100 (soft polymer), ~E/5 (cortical bone), E/2 (modified/soft titanium alloy), 2E (ceramic), 100E (imaginary material).

2.2 | Boundary conditions and interactions

Since the selected bone section is large enough with respect to the inserted implant in its middle, the boundary conditions on the far ends of the bone do not affect the local results near the implant, so that their sole role is to constrain rigid body motions. Thus, the distal side (where the Ramus is connected) was chosen to be fixed, while the mesial side was left free, as shown in Figure 1B.

Frictional contact (Coulomb friction) was assigned as the type of interaction for all the parts in in the model. A Ti-Ti coefficient of friction (COF = 0.36)[32] was assigned for the implant system parts (abutment, implant, and connecting screw), while the bone-implant interaction was assumed to be characterized by a coefficient of friction of 0.5 (COF = 0.5). This value is justified since the reported range of static coefficient of friction between bone and Titanium varies between COF = 0.39–1.00,[33] depending on the surface finish/roughness of the implant.

2.3 | Loading procedure

The loads were applied on the top of the abutment, Figure 1C. According to literature,[29,34,35] mastication loads exhibit a large variability in magnitude and direction. In order to recreate the failure envelope concept displayed in Ref. 24, the same loading procedure was adopted in this work, were the effect of the lateral and vertical loads combined and separate are presented. The procedure adopted was as follows:

Step 1: a prescribed fixed vertical load was applied to the top of the abutment (-y direction).

Step 2: the previous vertical load was kept, and a lateral load was applied (in the palatal direction, -x), increasing gradually up to the point cortical bone reached yielding or a predetermined octahedral shear strain magnitude, according to the selected failure criterion, as discussed in the sequel.

The prescribed fixed vertical range was: 0–50-100–150-200–300-400–500-600 N. In addition to a case of vertical load only, up to yield.

2.4 | Mesh

Tetrahedral elements, of type C3D4,[25] were used to mesh the parts of the model. A coarse mesh of typical element size of 0.6 mm was used for the abutment, since there was no particular interest in it. The connecting screw was meshed with typical element size of 0.2 mm. The same typical element size was used for the implant, with mesh refinements in the crestal bone-implant contact area. Far from the insertion hole, the bone was meshed with a coarser mesh of typical element size of 1.5 mm, while around the implant region, the mesh was refined to 0.2 mm typical element size, further refined near the neck of the implant (crestal bone) to 0.1 mm typical element size, to improve accuracy in that region of interest. Overall, 560 386 linear tetrahedral elements where used to mesh the model, as shown in Figure 1D,E.

2.5 | Failure criteria and calculated parameters

To calculate the failure envelopes,[24] Tresca stress yield criterion was chosen, with the following values: $\sigma_{y\ Tresca} = \frac{\sigma_{y\ Compression} - \sigma_{y\ Tension}}{2} = 135MPa$.[36]

In addition, the octahedral shear strain $\left(\varepsilon_{oct} = \frac{2}{3} \sqrt{(\varepsilon_1 - \varepsilon_2)^2 + (\varepsilon_2 - \varepsilon_3)^2 + (\varepsilon_3 - \varepsilon_1)^2} \right)$ was used as a criterion for the envelopes.[18] Admissible values for "normal" loading ranged from 1000 to 3000με. A "pathological" value of 10 000 με was also selected to provide additional information.

Characteristic values (Tresca stress or octahedral strain) were calculated by averaging the results over a particular region of interest (in the shape of a circular arc approximately 0.1 mm in depth (y), 0.2 mm in width (x), stretching 2 mm in length), located in the crestal bone, near the implant neck Figure 2 The values over that region were averaged to smoothen out any numerical artifact indicating excessively high local stress/strain values over a single element.

Bone displacements (micromotions) relative to the implant were extracted in the immediate vicinity of the implant, in both the lateral direction (-x), and inferior direction (-y), for a specific loading case (150 N vertical and 20 N lateral load) where the cortical bone did not yield
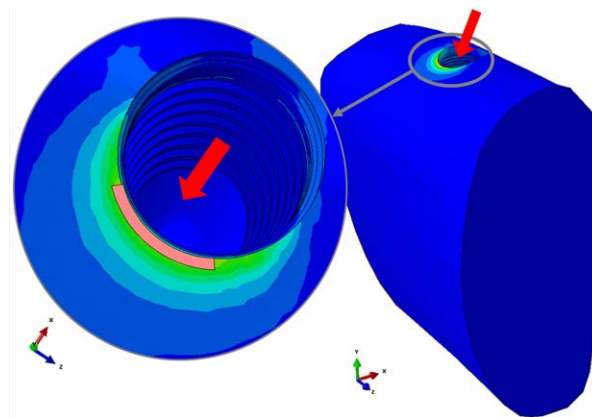

FIGURE 2 The region of interest (marked in pink) where the failure criteria were fulfilled. The arrows indicate the loading directions
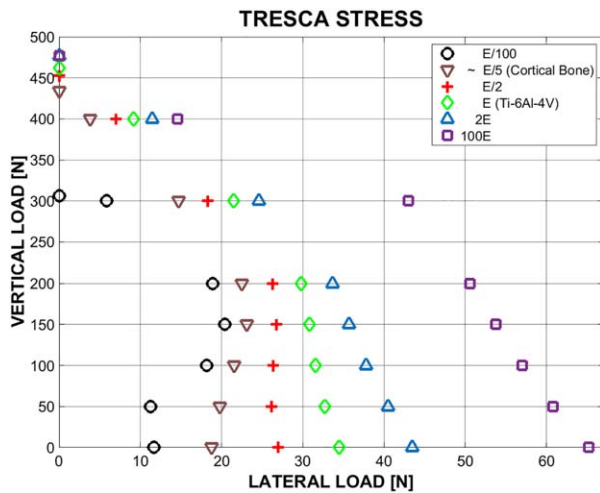
FIGURE 3 Tresca stress failure envelopes in the cortical bone for different Young's modulus of the implant system

for any of the selected Young's moduli cases. The rationale here was to identify the prescribed bone micromotions in the region of interest for the various cases of stiffness considered.

Finally, the octahedral shear strain distribution was extracted in the trabecular bone, for the specific loading case mentioned above in order to complement information retrieved for the cortical bone.

3 | RESULTS

3.1 | Tresca stress

Figure 3 shows the failure envelope according to Tresca (shear) stress in the cortical bone.

It can first be noted that the failure envelope expands laterally with increasing values of Young's modulus. This amounts to the fact that stiffer implants can bear higher loads before reaching cortical bone yielding. The shape of the envelopes changes for values above and below E/2. Above this "threshold," one can observe a noticeable increase in the lateral load, whereas below this value, the lateral load bearing capacity shrinks markedly, which indicates significant deflections in the implant itself. The very soft implant (E/100) has the smallest failure envelope. It is also interesting to note that the "bone-like" implant (~E/5) offers a relatively poor resistance to the lateral applied load. The vertical admissible load is not significantly affected by the implant's stiffness and has a characteristic value of 450 N.

3.2 | Octahedral shear strain

The failure envelopes corresponding to the octahedral shear are shown in Figure 4. Three different values are considered, namely 1000, 3000, and 10 000 με, respectively. While the first 2 values bound the domain of desired bone strains leading to bone remodeling according to the mechanostat model, the third value is representative of pathological strains that can lead to bone resorption.

First, one must keep in mind that the 1000 με envelope *must be exceeded* if bone resorption due to inactivity is to be avoided.

Concerning the lateral admissible load, the calculated values are small, and are probably achieved during normal mastication or other intra-oral activity. Looking at the vertical component, one can note that only 50–60 N are requested to keep the bone active. The overall influence of the Young's modulus is minimal, so that using material with higher Young's modulus probably will not lead to bone resorption due to strain shielding.
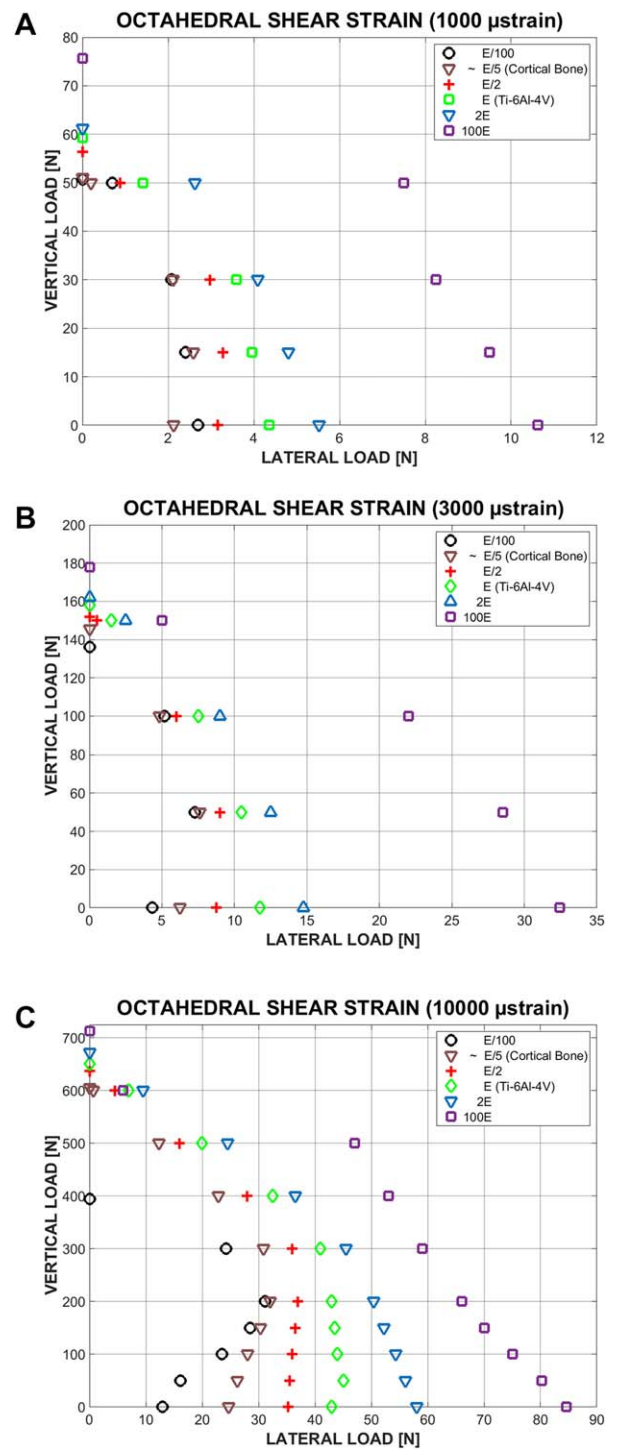

FIGURE 4 Octahedral shear strain failure envelopes in the cortical bone for different Young's moduli of the Implant system. A, 1000 με. B, 3000 με. C, 10 000 με
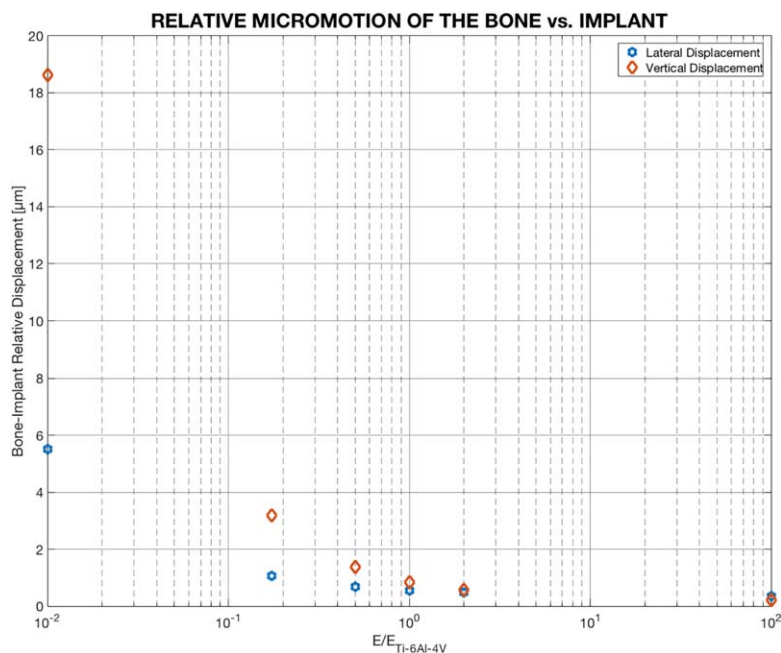
FIGURE 5 Lateral and vertical bone-implant micromotions near the crestal region

The 3000 $\mu\varepsilon$ envelope reveals a relative clustering of the admissible loads for all but the 100E stiffness case. Therefore, the upper strain range of the bone normal straining is relatively insensitive to the implant's material stiffness. The maximum normal load value of around 160 N is ideal for bone volume maintenance. When the lateral load is considered, the results indicate a beneficial increase of the admissible load with increasing stiffness values.

Considering the highest equivalent shear strain (10 000 $\mu\varepsilon$), one can notice again the same tendencies for the envelope evolutions that were observed for the Tresca shear stress criterion. Here too, the stiffer the implant, the higher the admissible loads that bring to this excessive strain value, which again indicates a beneficial effect of stiffer implants for cortical bone yielding. With that, one should note the relatively high value of the vertical load of 600–700 N.

3.3 | Horizontal and vertical bone-implant relative displacements

Figure 5 shows the calculated average bone displacement relative to the implant displacement in the region of interest for the various implant stiffness values.

A first observation is that the absolute value of the relative micromotions of the bone with respect to the implant are quite small, with a dominant vertical contribution. Here, it is important to remember that, contrary to the above failure envelopes, the calculated displacements correspond to only one loading case of 150 N vertical load and 20 N lateral load, noting that bone yielding has not occurred (considering Tresca stress failure envelopes) for this case irrespective of the material stiffness. The results clearly indicate that reduced implant stiffness induces larger relative micromotions as opposed to stiffer ones. Since relative micromotions are undesirable for the initial stages of

osseointegration, one can see a positive shielding effect of those micromotions, when the implant stiffness is increased.

3.4 | Trabecular bone strains

The trabecular shear strain corresponding to 150 N vertical and 20 N lateral loads is shown in Figure 6. Note that the scale bar is identical for all the studied case. As the material's stiffness increases, one can observe a non-monotonic increase of the near-apical strain. While the reasons for this non-monotonic behavior are not fully clear, one can surmise that the implant stiffness plays an important role on the overall peri-implant strains, with some balance between the coronal and apical parts which result in a complex strain pattern between the cortical and the trabecular bone components. This part of the study does not represent a comprehensive study of the trabecular bone strains as it only involves one loading case. With that, it should be noted that the maximum strain level is of the order of 1.2%, which is quite small for this kind of bone macrostructure.[29,30] Consequently, the outcome of this specific study justifies that the emphasis be put on the cortical bone, as in this work.

4 | DISCUSSION

This study aims at elucidating the role of the dental implant material's stiffness on the load transfer mechanism to the surrounding bone. This is done from the designer's perspective, according to which the admissible loads are calculated based on 2 specific bone failure criteria, embodied in the presented failure envelopes. Those are stress-based, namely bone yielding (Tresca criterion), strain-based to reflect the mechanostat approach which defines a range of admissible octahedral
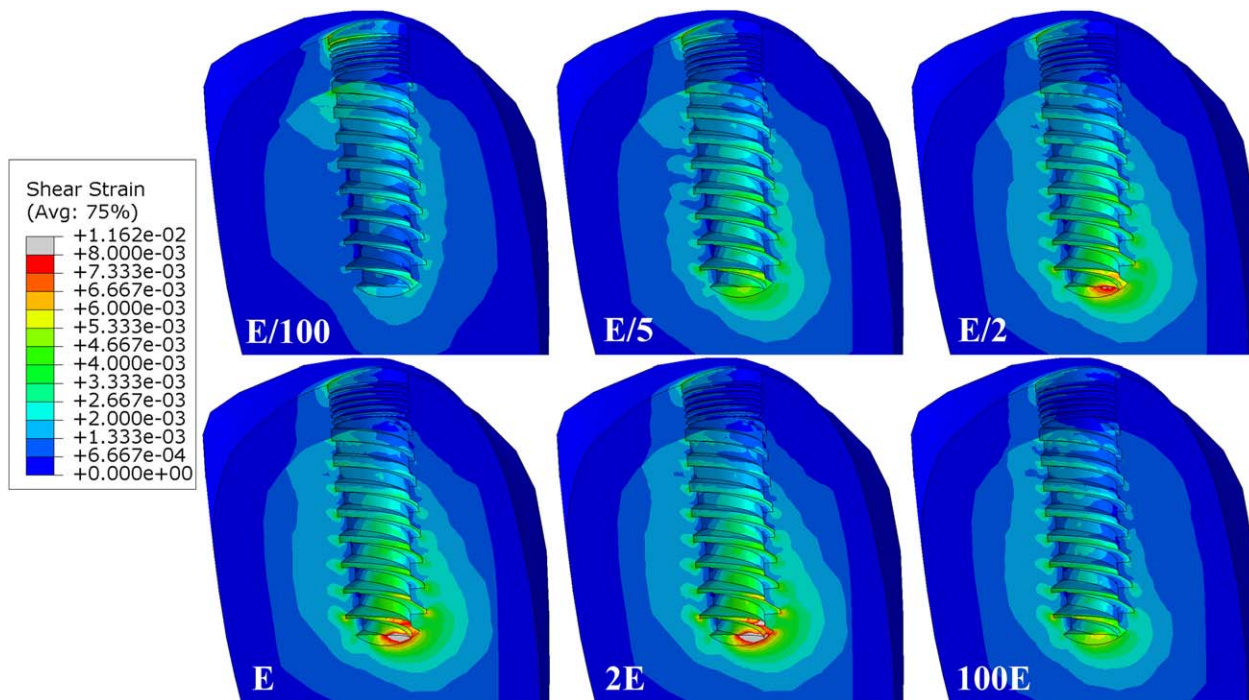
FIGURE 6 Shear strain in the trabecular bone for the different Young's moduli

shear strains between 1000–3000 $\mu\varepsilon$,[16] and finally consider bone-implant micromotions for a selected loading case.

While the implant geometry and interfacial coefficient of friction are identical in each loading case, the materials stiffness is systematically varied from that of Titanium toward 2 extremes, namely very soft (polymer) and very hard (imaginary) materials, including the realm of steels and ceramics, as well as cortical bone.

Before further discussion of the results, it is important to pay attention to the interfacial coefficient of friction. The latter represents the mechanical state of the interface and it was set to 0.5 in this work. In their previous study, Korabi and colleagues[24] examined various frictional cases for one fixed Young's modulus value (Titanium). Their results indicated that setting aside the extreme cases of non-frictional or fully bonded interface, variations in the coefficient of friction had a minimal effect on the failure envelope, with a tendency to shrink it as the coefficient of friction increased, as in the case of progressing osseointegration. The exact same trend is expected to apply to the present results concerning stress and strain-related failure envelopes, so that a value of 0.5 can be considered as representative.

Concerning, the bone-implant micromotions, it should be noted that there are no micromotions at a perfectly bonded interface, as noted by Refs. 4 and [5]. Here, the relative motion must be defined away from the interface to account for the deformability of both the bone and the implant. Such a procedure may be tricky and was not pursued here. Instead, we considered a frictional interface for which slippage is allowed, as a representation of the primary state of the bone-implant interface prior to full osseointegration, noting that even that stage dos not correspond to a fully bonded state, as noted by Refs. 4 and [5] and others.

Irrespective of the failure criterion, the failure envelope approach clearly showed that an increase in the implant's stiffness will allow for safe application of larger loads, with a minor influence over the vertical load component only.

We also examined the bone-implant micromotions for one specific load case and observed that the latter are very small, irrespective of the implant's stiffness.

Likewise, the strain experienced by the trabecular bone in the apical region remains bounded and quite small irrespective of the implant's material.

Throughout the work, we could not pinpoint any kind of shielding effect over the stress, strain or micromotions. Contrary to the accepted paradigm, our study shows that higher stiffness implants are not only harmless to the jawbone but may even be beneficial in term of work loads.

While the 100E material does not exist, the E/100 material which corresponds to a polymeric implant was found to be the worst performer in this study. This is most likely because this material is more compliant than the bone itself and therefore "suffers" much more than the bone, and in that respect, polymers do not seem to be the best choice for dental implant materials.

Likewise, this study shows that one should not be reluctant to consider ceramic materials on the one hand, but also that investing in the development of more compliant implant materials is not justified by the results of our study.

At this stage, it should be noted that this study considers single-material implants with a well-defined stiffness. In view of the present results, it might be interesting to consider functionally graded materials (and perhaps geometries) that would be optimized to suit a selected failure envelope (or set of for strain-based criteria). The benefit of such

graded materials has been demonstrated for orthopedic applications,[37,38] and their potential for dental applications deserves investigation using the failure envelope concept.

5 | CONCLUDING REMARKS

The influence of the dental implant materials' stiffness on their functionality was characterized using failure envelopes, in which both stress, strain and displacement-based failure criteria were considered for the cortical bone.

The failure envelope concept allows for a general characterization of the implants functionality for all possible combinations of applied loads and directions.

For stress/strain-based failure criteria, the calculations indicate that the stiffer materials allow for wider failure envelopes, and thus increased implant functionality.

As a result, matching the bone's compliance for the implant's material offers no advantage with respect to stiffer materials. On the contrary.

For very soft materials such as polymers, the failure envelope shrinks to its bare minimum due to excessive implant distortion, which is undesirable.

As the implant's compliance increases, the trabecular bone experiences smaller strains. However, whatever the implant's stiffness, the trabecular strains remain small.

When bone-implant micromotions are considered, higher stiffness implants are preferable as they reduce the calculated displacement values, even if the latter remain overall quite small.

This study contradicts the paradigm stating that higher compliance materials are preferable for dental implants, based on shielding assumptions, and in fact just points to the opposite.

The present results do not support the concept of stress, strain or displacement shielding for the bone-dental implant system.

CONFLICT OF INTEREST

All authors state that they have no conflicts of interest with respect to this work.

REFERENCES

[1] Huiskes R, Weinans H, van Rietbergen B. The relationship between stress shielding and bone resorption around total hip stems and the effects of flexible materials. *Clin Orthop Relat Res.* 1992;(274):124–134. doi:10.1097/00003086-199201000-00014

[2] Kuiper J, Huiskes R. The predictive value of stress shielding for quantification of adaptive bone resorption around hip replacements. *J Biomech Eng.* 1997;119:228–231.

[3] Skerry TM. The response of bone to mechanical loading and disuse: fundamental principles and influences on osteoblast/osteocyte homeostasis. *Arch Biochem Biophys.* 2008;473:117–123.

[4] Mathieu V, Vayron R, Richard G, et al. Biomechanical determinants of the stability of dental implants: influence of the bone-implant interface properties. *J Biomech.* 2014;47:3–13.

[5] Haïat G, Wang H-L, Brunski J. Effects of biomechanical properties of the bone-implant interface on dental implant stability: from in silico approaches to the patient's mouth. *Annu Rev Biomed Eng.* 2013;16:187–213.

[6] Cilla M, Checa S, Duda GN. Strain shielding inspired re-design of proximal femoral stems for total hip arthroplasty. *J Orthop Res.* 2017. doi:10.1002/jor.23540

[7] Lee W-T, Koak JY, Lim YJ, Kim SK, Kwon HB, Kim MJ. Stress shielding and fatigue limits of poly-ether-ether-ketone dental implants. *J Biomed Mater Res B Appl Biomater.* 2012;100:1044–1052.

[8] Meireles S, Completo A, António Simões J, Flores P. Strain shielding in distal femur after patellofemoral arthroplasty under different activity conditions. *J Biomech.* 2010;43:477–484.

[9] Sumitomo N, Noritake K, Hattori T, et al. Experiment study on fracture fixation with low rigidity titanium alloy: plate fixation of tibia fracture model in rabbit. *J Mater Sci Mater Med.* 2008;19:1581–1586.

[10] Özcan M, Hämmerle C. Titanium as a reconstruction and implant material in dentistry: advantages and pitfalls. *Materials (Basel).* 2012;5:1528–1545.

[11] Rouhi G, Tahani M, Haghighi B, Herzog W. Prediction of stress shielding around orthopedic screws: time-dependent bone remodeling analysis using finite element approach. *J Med Biol Eng.* 2015;35:545–554.

[12] Najeeb S, Zafar MS, Khurshid Z, Siddiqui F. Applications of polyetheretherketone (PEEK) in oral implantology and prosthodontics. *J Prosthodont Res.* 2016;60:12–19.

[13] Asgharzadeh Shirazi H, Ayatollahi MR, Asnafi A. To reduce the maximum stress and the stress shielding effect around a dental implant-bone interface using radial functionally graded biomaterials. *Comput Methods Biomech Biomed Engin.* 2017;20:750–759.

[14] Wiskott H, Belser U. Lack of integration of smooth titanium surfaces: a working hypothesis based on strains generated in the surrounding bone. *Clin Oral Implants Res.* 1999;10:429–444.

[15] Wolff J. *The Law of Transformation of Bones.* Berlin: Verlag Von August Hirschwald; 1892.

[16] Frost HM. Wolff's Law and bone's structural adaptations to mechanical usage: an overview for clinicians. *Angle Orthod.* 1994;64:175–188.

[17] Frost HM. A 2003 update of bone physiology and Wolff s law for clinicians. *Angle Orthod.* 2004;74:3–15.

[18] Piccinini M, Cugnoni J, Botsis J, Ammann P, Wiskott A. Numerical prediction of peri-implant bone adaptation: comparison of mechanical stimuli and sensitivity to modeling parameters. *Med Eng Phys.* 2016;38:1348–1359.

[19] Osman R, Swain M. A critical review of dental implant materials with an emphasis on titanium versus zirconia. *Materials (Basel).* 2015;8:932–958.

[20] Stoppie N, Van Oosterwyck H, Jansen J, Wolke J, Wevers M, Naert I. The influence of Young's modulus of loaded implants on bone remodeling: an experimental and numerical study in the goat knee. *J Biomed Mater Res A.* 2009;90:792–803.

[21] Valiev RZ, Estrin Y, Horita Z, Langdon TG, Zechetbauer MJ, Zhu YT. Producing bulk ultrafine grained materials by severe plastic deformation. *JOM.* 2006;58:33–39.

[22] Vaillancourt H, Pilliar RM, McCammond D. Finite element analysis of crestal bone loss around porous-coated dental implants. *J Appl Biomater.* 1995;6:267–282.

[23] Piotrowski B, Baptista AA, Patoor E, Bravetti P, Eberhardt A, Laheurte P. Interaction of bone-dental implant with new ultra low

modulus alloy using a numerical approach. *Mater Sci Eng C Mater Biol Appl.* 2014;38:151–160.

[24] Korabi R, Shemtov-Yona K, Dorogoy A, Rittel D. The failure envelope concept applied to the bone-dental implant system. *Sci. Rep.* 2017;7:2051.

[25] Simulia. *Abaqus/CAE Version 6.14–2*. Providence, RI: Dassault Systèmes Simulia Corp.; 2014.

[26] Human Jaw - Recent Models - GrabCAD - CAD Library. https://grab-cad.com/library?query=human jaw. Accessed December 20, 2015

[27] Farnsworth D, Rossouw PE, Ceen RF, Buschang PH. Cortical bone thickness at common miniscrew implant placement sites. *Am. J. Orthod. Dentofacial Orthop.* 2011;139:495–503.

[28] Schwartz-Dabney CL, Dechow PC. Variations in cortical material properties throughout the human dentate mandible. *Am J Phys Anthropol.* 2003;120:252–277.

[29] Misch CE, Qu Z, Bidez MW. Mechanical properties of trabecular bone in the human mandible: implications for dental implant treatment planning and surgical placement. *J Oral Maxillofac Surg.* 1999; 57:700–706.

[30] Lakatos E, Magyar L, Bojtár I. Material properties of the mandibular trabecular bone. *J Med Eng.* 2014;2014:470539.

[31] American Society for Testing and Materials. *Standard Specification for Wrought Titanium-6Aluminum-4Vanadium ELI (Extra Low Interstitial) Alloy for Surgical Implant Applications (UNS R56401)*. ASTM Int'l., West Conshohoken, PA 2003, 2013.

[32] American Society for Testing and Materials. *ASTM-G98*. West Conshohoken, PA: ASTM Int'l.; 2003.

[33] Grant JA, Bishop NE, Götzen N, Sprecher C, Honl M, Morlock MM. Artificial composite bone as a model of human trabecular bone: the implant-bone interface. *J Biomech.* 2007;40:1158–1164.

[34] Misch CE. *Contemporary Implant Dentistry*. Maryland Heights, MO: Elsevier Health Sciences; 2008.

[35] Brunski J, Puleo D, Nanci A. Biomaterials and biomechanics of oral and maxillofacial implants: current status and future developments. *Int J Oral Maxillofac Implants.* 2000;15(1):15–46.

[36] Natali AN. *Dental Biomechanics*. New York: CRC Press; 2003. doi: 10.1201/9780203514849

[37] Gefen A. Computational simulations of stress shielding and bone resorption around existing and computer-designed orthopaedic screws. *Med Biol Eng Comput.* 2002;40:311–322.

[38] Gefen A. Optimizing the biomechanical compatibility of orthopedic screws for bone fracture fixation. *Med Eng Phys.* 2002;24:337–347.